Am J Transl Res 2019;11(5):2725-2741
www.ajtr.org /ISSN:1943-8141/AJTR0087913

Original Article

P-AKT2/SPK1 (P-SPK1) and P-MEK/P-ERK cell signaling pathways are involved in LPS-induced macrophage migration

Yonghong Lei[2*], Yanping Yang[1*], Jieqiong Zhao[1], Haibo Gao[1], Ruirui Chen[1], Baobao Bai[1], Xiaohui Kang[1], Yong He[1], Lu Ding[1], Ting Wei[1], Xiaobing Fu[2], Lianyou Zhao[1], Xue Li[1]

[1]Department of Cardiology, Tangdu Hospital, Xi'an 710038, Shaanxi, China; [2]Department of Plastic Surgery, 301 Hospital, Beijing 100001, China. [*]Co-first authors.

Received November 5, 2018; Accepted March 23, 2019; Epub May 15, 2019; Published May 30, 2019

Abstract: Macrophage recruitment to the inflammation site is essential for LPS-induced myocarditis, although the underlying mechanism remains elusive. This study was designed to examine the role of the P-AKT2/SPK1 (P-SPK1) and P-MEK/P-ERK signaling cascades in the regulation of macrophage migration and LPS-induced myocarditis. Our data revealed that (1) the P-AKT2/SPK1 (P-SPK1) and P-MEK/P-ERK signaling cascades acted separately in the regulation of macrophage migration; (2) P-AKT2/SPK1 (P-SPK1) played a relatively important role compared to P-MEK/P-ERK cell signaling in LPS-induced macrophage migration; (3) atorvastatin (ATV) inhibited macrophage migration by inhibiting P-AKT2/SPK1 (P-SPK1) cell signaling, but ATV could increase P-MEK and P-ERK protein expression; (4) ATV has a beneficial effect on LPS-induced myocarditis via inhibition of P-AKT2/SPK1-mediated macrophage recruitment, apoptosis, TNFα, IL-1β, and IL-6; (5) ATV-offered protection against LPS-induced myocarditis was eliminated from SPK1-KO mice; (6) SPK1 may play a harmful role in LPS-induced myocarditis. Taken together, our data revealed that SPK1 represents a novel regulating factor for macrophage migration and cardiac protection under LPS-induced myocarditis.

Keywords: Macrophage migration, P-SPK1, P-MEK/P-ERK, macrophage recruitment

Introduction

Macrophages are important mediators of inflammatory cardiovascular diseases. Experiments show that inflammatory cardiovascular diseases are characterized by pronounced macrophage infiltration [1]. In our previous study, we found that AKT (Protein kinase B) regulated macrophage migration and was closely related to cardiac remodeling after ischemia injury [2]. Zhou *et al.* demonstrated that MEK (Mitogen-activated protein/extracellular signal-regulated kinase) and ERK1/2 (Extracellular signal-regulated kinase) were also involved in macrophage migration [3]. The relationship between MEK/ERK and P-AKT2/SPK1 (Sphingosine kinase 1) cell signaling during LPS (Lipopolysaccharide)-induced macrophage migration, in which cell signaling plays an important role, and how ATV affects the MEK/ERK and P-AKT2/SPK1 cell signaling pathway are not well understood. To this end, our study was designed: (1) to determine the relationship between MEK/ERK and P-AKT2/SPK1 in LPS-induced macrophage migration; (2) to determine which cell signaling pathway (AKT2/SPK1 or MEK/ERK) is more important during macrophage migration; (3) to investigate the effect of ATV on MEK/ERK and P-AKT2/SPK1 cell signaling; (4) to determine if SPK1 is harmful in the LPS induced myocarditis model.

Materials and methods

Animal model

SPK1-/- [4] and AKT2-/- [5] mice were obtained from the Jackson Laboratory (Bar Harbor, ME, USA). SPK1-/- and AKT2-/- mice were engineered on a C57BL/6 background. Non-transgenic mouse litters served as controls, and all mice used were 8 to 12-week-old male mice. Mice

were fed with ATV at 10 mg/kg/day (Sigma Aldrich, St. Louis, MO, USA) by gastric gavage for 1 week before and after LPS induction. All animal procedures were carried out according to National Institutes of Health Guide for the Care and Use of Laboratory Animals guidelines and were approved by the Animal Care and Use Committee of the Fourth Military Medical University, Xi'an, China.

Antibodies

Antibodies were directed against SPK1 (DBA Acris Antibodies, Rockville, MD, USA), P-SPK1 (DBA Acris Antibodies), ERK (Abcam, Cambridge, MA, USA), P-ERK (Abcam, Cambridge, MA, USA), AKT2 (Abcam, Cambridge, MA, USA), P-AKT2 (Abcam, Cambridge, MA, USA), goat anti-rabbit IgG H&L (Abcam, Cambridge, MA, USA), Caspase-8 (Abcam, Cambridge, MA, USA), IL-6 (Abcam, Cambridge, MA, USA), GAPDH (Abcam, Cambridge, MA, USA), F4/80 (Santa Cruz Biotechnology, Santa Cruz, CA, USA), and donkey anti-goat IgG-HRP (Santa Cruz Biotechnology, Santa Cruz, CA, USA), Caspase 3 (Proteintech Group, Inc., Chicago, IL, USA), MEK (Cell Signaling Technology, Danvers, MA, USA), and P-MEK (Cell Signaling Technology, Danvers, MA, USA).

Materials

Isoproterenol were obtained from Hospira (Hospira, UT, USA). LPS and atorvastatin calcium salt trihydrate were obtained from Sigma Aldrich (St. Louis, MO, USA). The ANA-1 cell line was obtained from the Cell Bank of the Chinese Academy of Sciences. Transwells were purchased from Corning Costar Company (Cambridge, MA, USA).

Isolation of murine peritoneal macrophages

Peritoneal macrophages were isolated from wild type (WT) or SPK1-/- mice, according to established protocols [6]. Briefly, after mice were euthanized by cervical dislocation, the body was cleaned with 75% ethanol, a small incision was made in the abdomen, and mice were injected with 10 mL 1×PBS (Polybutylene Succinate) through the peritoneal wall into the peritoneal cavity, without puncturing the intestine or any other organ. Peritoneal fluid was collected as completely as possible into a 15 mL tube and centrifuged at 800 g at 4°C for 5 min. The pellets containing cells were washed twice and resuspended in DMEM (Dulbecco's Modified Eagle Medium)/F12 with 10% FBS (Fetal Bovine Serum), 50 μg/ml gentamicin, 50 μg/ml penicillin, and 50 ug/ml streptomycin. The fluid was plated in a 60 mm dish and allowed to attach for 2 h in a humidified incubator with 5% CO_2 at 37°C. Non-adherent cells were removed by vigorously washing three times with ice-cold PBS. Adherent cells were cultured for another 24 h for other experiments.

SPK1 and MEK lentivirus and cell transfection

Production of knockdown SPK1 and MEK lentivirus vectors was performed as previously described [7]. An GFP-encoding lentiviral strain was created containing the siRNA oligonucleotides that targets 5'-GGCAGAGATAACCTTTAAA-3' on SPK1 mRNA, MEK1-siRNA oligonucleotides that target 5'-GAGGCCTTTCTGACGCAGAAGCAGAA-3', and MEK2-siRNA 5'-CGGTGTTACCGGCACTCACTATCAA-3' (Gene Chem, Shanghai, China). A scramble siRNA with the sequence 5'-TTCTCCGAACACGTGTCACGT-3' was cloned in parallel to create the negative control lentiviral strain. The titer of the SPK1-siRNA and negative control were approximately 8×10^8 TU/ml and 5×10^8 TU/ml of the MEK-siRNA. 3-5×10^4/ml ANA-1 cells (Chinese Academy of Sciences, Shanghai, China) were seeded in each well of a 6-well plate and cultured 24 h until 30-40% of them fused. Cells were starved for 24 h, and lentiviral stocks were diluted to MOI 20 with enhanced infection solution (Gene Chem) containing polybrene (5 ug/ml) added to infect the seeded cells for 12 h with FBS-free RPMI-1640. The virus-containing medium was then replaced with fresh RPMI-1640 medium containing 10% FBS. Three days after infection, the expression of the reporter gene in the lentivirus was observed via green fluorescent protein (GFP). Fluorescence microscopy (IX-53; Olympus Corporation, Tokyo, Japan) was used to detect cells expressing green fluorescence, and the percentage of GFP-positive cells was used to measure the infection efficiency of the cells.

Macrophage migration

Cell migration was performed in a 24-well transwell migration system (Corning Costar) as previously described [8]. For the cell migration assay, cells were pre-treated with ATV (10 uM)

for 24 h at 37°C. Cells were then harvested, suspended in serum-free medium, and added to the upper transwell chambers at a density of 5×10^5 cells per chamber. Serum-free medium with LPS (100 ng/ml) was added in the lower chamber. After 12 h incubation, the insert was removed, and cells were scraped from the upper surface with a cotton swab. Cells on the lower surface were fixed with 4% paraformaldehyde in PBS for 30 min and permeabilized with 0.2% Triton X-100 in PBS for 5 min, and then stained with DAPI (4',6-diamino-2-phenylindole dihydrochloride, Molecular Probes). The stained cells were photographed and counted using Image-Pro Plus Software. Total nuclei (DAPI staining, blue) in each field were counted by IP Lab Imagine Analysis Software (Version 3.5; Scanalytics, Fairfax, VA, USA). Results from different fields from the same slide were averaged and counted as one sample.

Real-time quantitative polymerase chain reaction

Real-time quantitative polymerase chain reaction analysis determined gene expression. Briefly, reverse-transcribed cDNA from myocardial RNA was used to determine gene expression. Real time PCR was performed in a 50-l reaction (40 ng of genomic DNA, 250 nM each primer, 1×SYBR Green Master Mix). Each experimental group was performed in triplicate. The CT method using GAPDH as a reference gene was used to quantify the results and perform statistical analysis as previously described [9]. CT values were then converted to fold changes in gene expression relative to WT samples. Mouse gene specific primer sets were as follows: ANP sense 5'-CGTGCCCCGACCCACGCCAGCATGG-3' and anti-sense 5'-GCCTCCGAGGGCCAGCGAGCAGAGC-3'; TNFα sense 5'-CACAGAAAGCATGATCCGCGACGT-3' and anti-sense 5'-CGGCAGAGAGGAGGTTGACTTTCT-3'; IL-1β sense 5'-GCTGCTTCCAAACCTTTGAC-3' and antisense 5'-AGCTTCTCCACAGCCACAAT-3'; GAPDH sense 5'-AACGACCCCTTCATTGAC-3' and antisense 5'-TCCACGACATACTCAGCAC-3'.

Animal LPS-induced myocarditis model and ATV treatment

The LPS-induced myocarditis animal model has been previously described [10]. Mice were randomly assigned to six groups: WT Control (WT mice without LPS induction), WT LPS (WT mice with LPS induction), WT LPS+ATV (WT mice with LPS and ATV induction), SPK1-/- Control (SPK1-/- mice without LPS induction), SPK1-/- LPS (SPK1-/- mice with LPS induction), or SPK1-/- LPS+ATV (SPK1-/- mice with LPS and ATV induction). Mice were fed ATV (10 mg/kg/day) for 7 days, and the LPS induced myocarditis procedure was performed. Seven days after this LPS-induced myocarditis, mice were again treated with ATV for 7 days.

Echocardiography

We assessed *in vivo* cardiac function at 4 weeks after MI by using an echocardiographic imaging system (Vevo 770, VisualSonic, Toronto, Canada). Mice were anesthetized with 1.5% isoflurane and two-dimensional echocardiographic views of the mid-ventricular short axis were obtained at the level of the papillary muscle tips below the mitral valve. LV internal dimensions were measured and the LV fractional shortening (LVFS) was calculated as previously described [11].

Hemodynamic analysis of cardiac function

For *in vivo* hemodynamic measurements, a 1.4 French micro-manometer-tipped catheter (SPR-671; Millar Instruments Inc., Houston, TX, USA) was inserted into the right carotid artery and advanced into the left ventricle (LV) of mice that were lightly anesthetized (*i.e.* maintained spontaneous respirations) with tribromoethanol/amylene hydrate (2.5% w/v, 8 µl/g injected intraperitoneally; Avertin (Sigma-Aldrich, Steinheim, Germany). Hemodynamic parameters, including heart rate, LV end-diastolic pressure, and +dP/dt and -dP/dt were recorded in closed-chest mode, both at baseline and in response to isoproterenol (10 ng), administered via cannulation of the right internal jugular vein [12].

Immunoblotting

Immunoblots were performed according to established methods [13]. LV tissue was homogenized in 10 volumes of lysis buffer (50 mM Tris-HCl, pH 7.4), 150 mM NaCl, 1 mM EDTA, 0.25% sodium deoxycholate, and 1% NP-40 with a protease inhibitor cocktail and phosphatase inhibitor cocktail. After homogenization, the homogenates were centrifuged at 15,000×g for 15 min and separated into

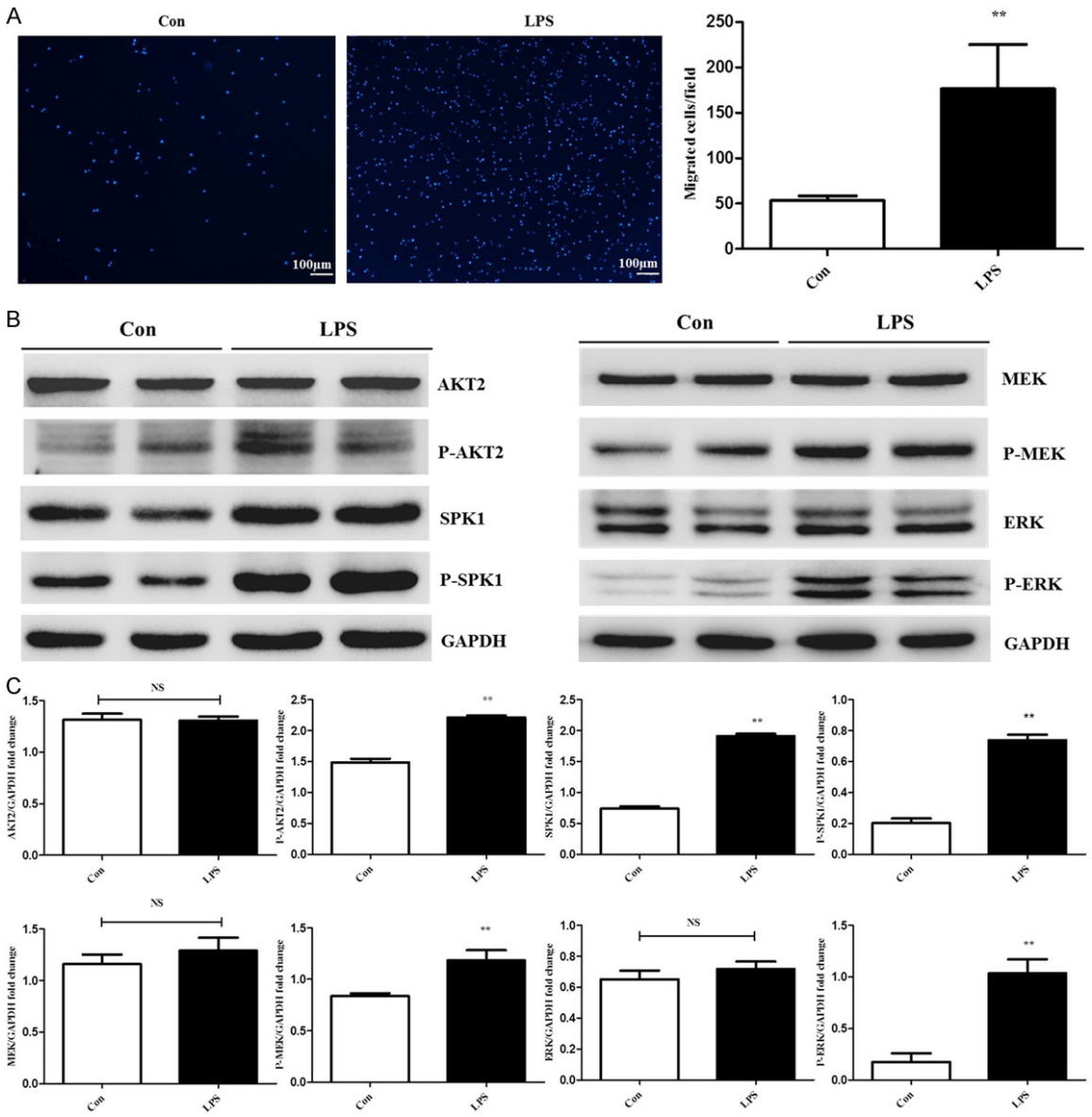

Figure 1. LPS increases ANA-1 cell migration and P-AKT2, SPK1, P-SPK1, P-MEK, and P-ERK protein expression. A. LPS increased migration of ANA-1 cells in a trans-well assay. Cells were grown overnight, starved for 24 h, and detached. 5×10^5 cells were plated in the upper well in a serum-free RPMI 1640 medium containing 100 ng/ml LPS. After 16 h of incubation, cells migrating across the membrane were stained and counted. Four random fields were counted, and the number of migrated cells was used as an index for migration. The experiment was repeated three times. B. Protein expression in LPS induced ANA-1 cells. Whole cell lysates were prepared after cells were starved for 24 h and stimulated with 100 ng/ml LPS for 2 h. Immunoblots shows total AKT2, P-AKT2, SPK1, P-SPK1, MEK, P-MEK, ERK, P-ERK, and GAPDH protein expression levels. C. GAPDH normalized AKT2, P-AKT2, SPK1, P-SPK1, MEK, P-MEK, ERK, and P-ERK levels. Data are presented as the mean ± SEM.; n=3. *P < 0.05, **P < 0.01 compared with Con (Control); NS = not significant.

NP-40-soluble supernatant and insoluble pellets. Equal amounts of proteins were subjected to SDS-PAGE (Sodium Dodecyl Sulphate-Polyacrylamide Gel Electrophoresis) and were subsequently transferred to nitrocellulose membranes. Membranes were scanned with the Odyssey Infrared Imaging System (LI-COR, Lincoln, Nebraska, USA).

Immunohistochemical staining

Tissue sections (4-5 μm) were deparaffinized and dehydrated using a graded series of ethanol solutions and stained with F4/80. Endogenous peroxidase was then inactivated with 3% hydrogen peroxide at room temperature for 20 min. Slides were soaked in a 0.1 mol/L

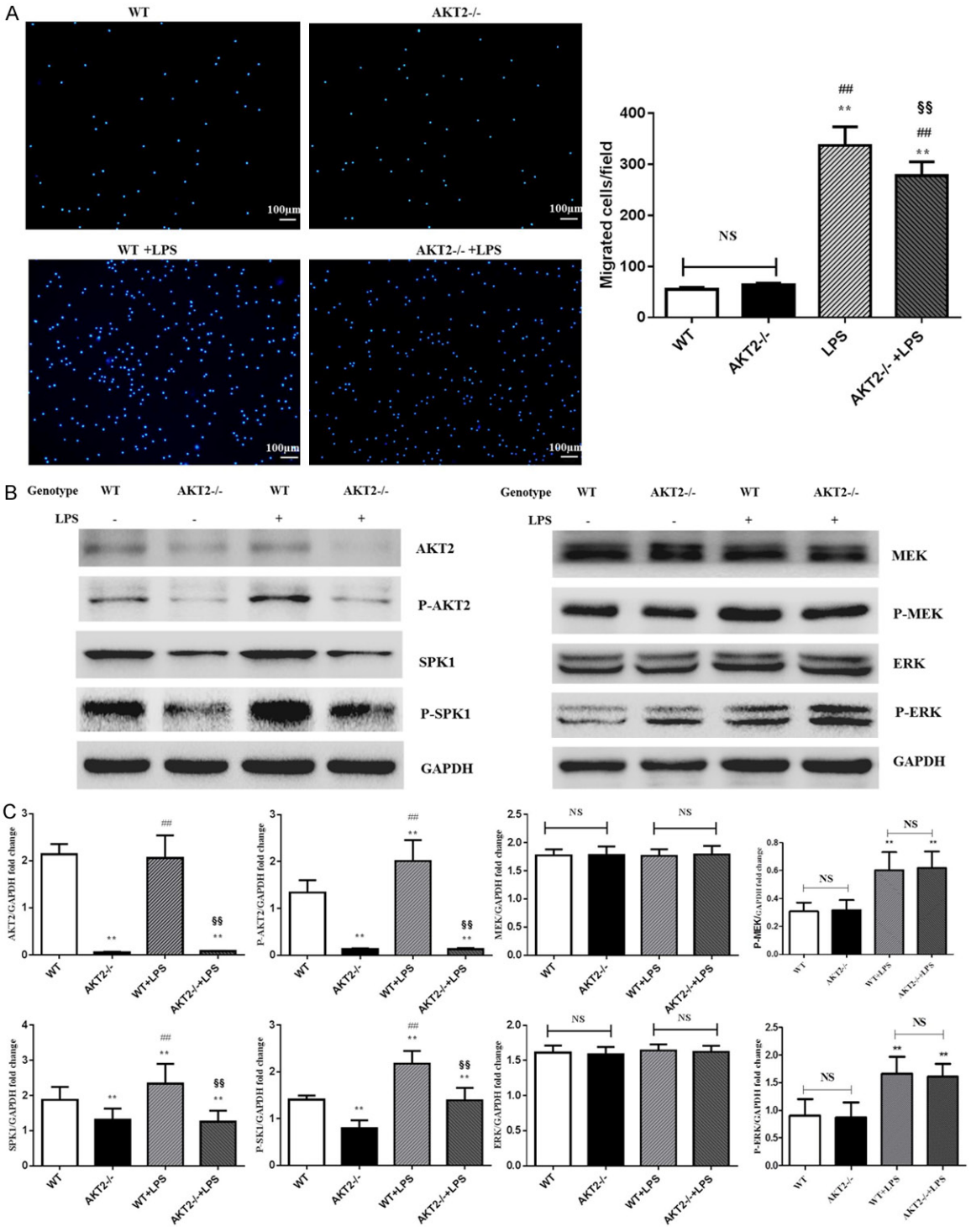

Figure 2. Macrophage migration and levels of AKT2, P-AKT2, SPK1, P-SPK1, MEK, P-MEK, ERK, and P-ERK in LPS induced murine peritoneal macrophages from WT and AKT2 KO (AKT2-/-) mice. A. Migration of peritoneal macrophages from WT and AKT2-/- mice. Primary cells enriched for macrophages were placed into 6-well plates (1×10^6 cells/ml) in DMEM plus 10% FBS. After 24 h incubation and starving overnight, cells were plated in the upper well and serum-free RPMI 1640 medium containing 100 ng/ml LPS was added to the bottom well. After 16 h of incubation, cells migrating across the membrane were stained and counted. Four random fields were counted, and the number of migrated cells was used as an index for migration. B. Protein expression in LPS induced murine peritoneal macrophages. Whole cell lysates were prepared after cells were stimulated with LPS. Immunoblots show total AKT2, P-AKT2, SPK1, P-SPK1, MEK, P-MEK, ERK, P-ERK, and GAPDH protein expression levels. C. GAPDH normalized AKT2, P-AKT2, SPK1, P-SPK1, MEK, P-MEK, ERK, and P-ERK levels. Data are presented as the mean ± SEM, n=3. *P < 0.05, **P < 0.01 compared with WT without LPS; #P < 0.05, ##P < 0.01 compared with AKT2-/- group; §P < 0.05, §§P < 0.01 compared with WT+LPS induced group. NS = not significant.

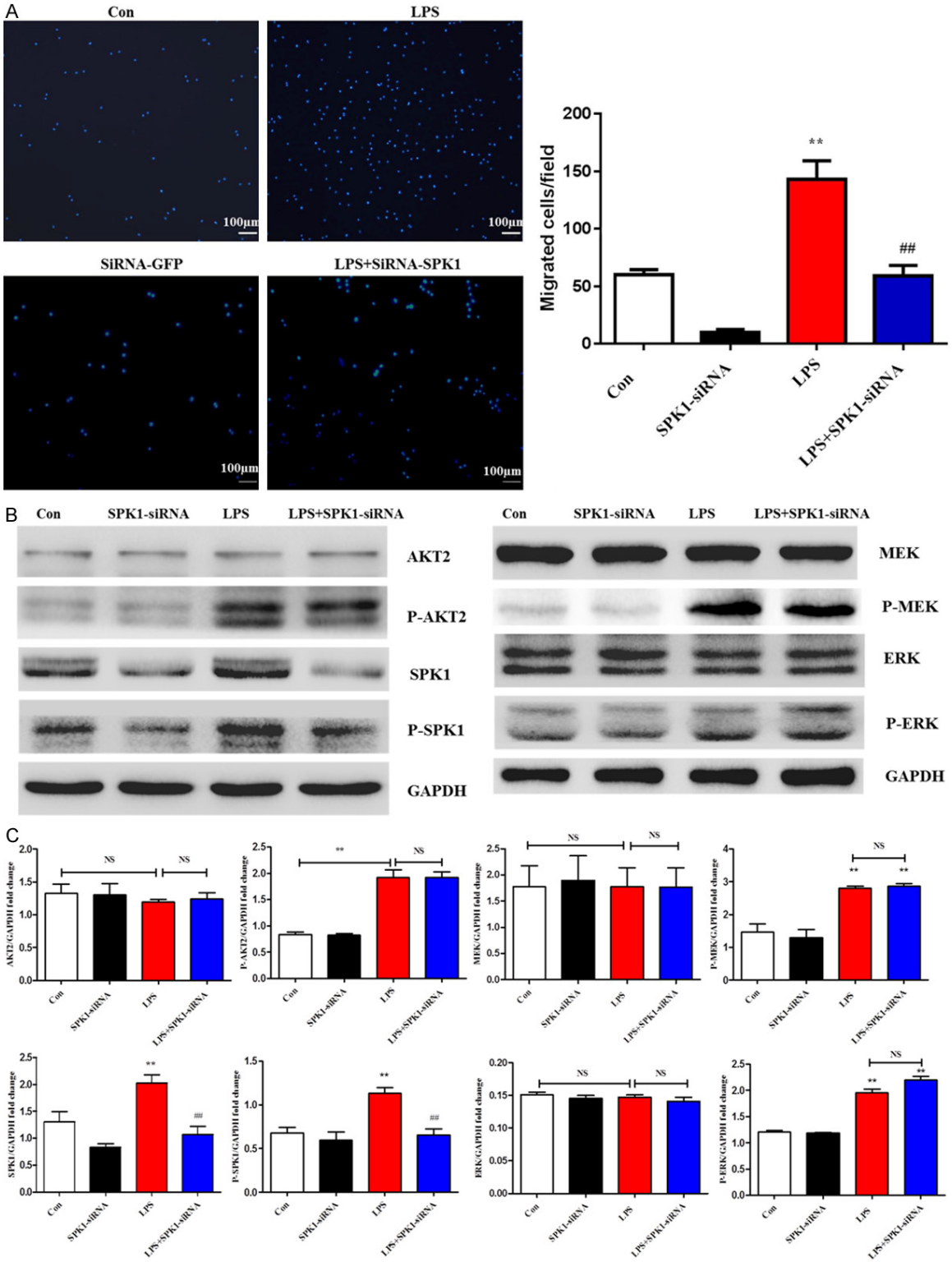

Figure 3. SPK1-siRNA decreased ANA-1 cell migration and SPK1 and P-SPK1 protein expression, but had no effect on protein levels of AKT2, P-AKT2, MEK, P-MEK, ERK, and P-ERK. A. SPK1-siRNA decreased migration of ANA-1 cells in a trans-well assay after LPS induction. ANA-1 cells were infected by LV-SPK1-siRNA, then cells were detached and cell suspension (5×10^5 cells/ml) was placed in the upper well and serum-free RPMI 1640 medium with 100 ng/ml LPS was added to the bottom well. After 16 h of incubation, cells migrating across the membrane were stained and counted. The experiment was repeated three times. B. Protein expression in LPS and SPK1-siRNA induced ANA-1 cells. Whole cell lysates were prepared following stimulation with LPS and SPK1-siRAN. Immunoblots showed AKT2, P-AKT2, SPK1, P-SPK1, MEK, P-MEK, ERK, P-ERK, and GAPDH protein expression levels. C. GAPDH normalized lev-

els of AKT2, P-AKT2, SPK1, P-SPK1, MEK, P-MEK, ERK, and P-ERK. Data are presented as the mean ± SEM; n=3. *P < 0.05, **P < 0.01 compared with Con without LPS; #P < 0.05, ##P < 0.01 compared with the Con+LPS induced group; NS = not significant.

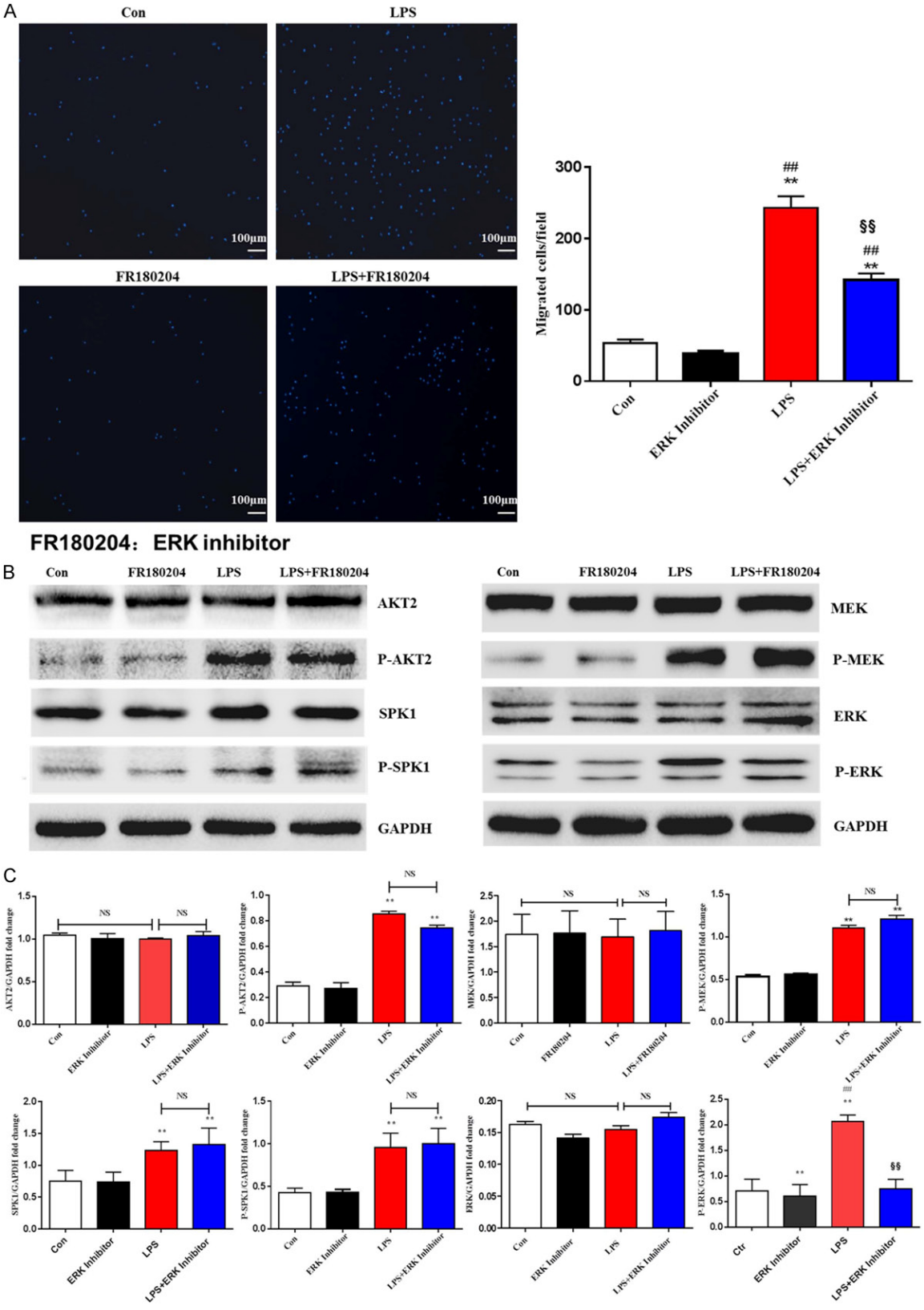

Figure 4. ERK inhibitor decreased ANA-1 cell migration and ERK and P-ERK protein expression, but had no effect on protein levels of AKT2, P-AKT2, SPK1, P-SPK1, MEK, P-MEK, ERK, and P-ERK. A. ERK inhibitor decreased migration of ANA-1 cells in a trans-well assay after LPS induction. ANA-1 cells were infected by ERK inhibitor FR180204, then cells were detached and cell suspension (5×10^5 cells/ml) was placed in the upper well and serum-free RPMI 1640 medium with 100 ng/ml LPS was added to the bottom well. After 16 h of incubation, cells migrating across the membrane were stained and counted. The experiment was repeated at least three times with similar results. B. Protein expression in LPS and ERK inhibitor FR180204 induced ANA-1 cells. Whole cell lysates were prepared following stimulation with LPS and ERK inhibitor. Immunoblots showed AKT2, P-AKT2, SPK1, P-SPK1, MEK, P-MEK, ERK, P-ERK, and GAPDH protein expression levels. C. GAPDH normalized levels of AKT2, P-AKT2, SPK1, P-SPK1, MEK, P-MEK, ERK, and P-ERK. Data are presented as the mean ± SEM; n=3. *P < 0.05, **P < 0.01 compared with Con without LPS; #P < 0.05, ##P < 0.01 compared with ERK inhibitor FR180204 induced group; §P < 0.05, §§P < 0.01 compared with Con+LPS induced group; NS = not significant.

citrate buffer (pH 6.0) and placed in an autoclave at 121°C for 2 min for antigen retrieval. After washing with PBS (pH 7.4), the sections were blocked with 1% BSA diluted in PBS at 37°C for 30 min, and then incubated with anti-F4/80 (1:50, Abcam, Cambridge, UK) at 4°C overnight. After being rinsed with PBS again, the sections were incubated with HRP-conjugated goat anti-mouse antibody and DAB (DAKO, Glostrup, Denmark), washed with distilled water, incubated with 0.5% PAS for 10 min in a dark chamber, and washed again with distilled water for 3 min. Finally, sections were counter stained with hematoxylin. All sections with immunohistochemical staining were observed and photographed with an Olympus microscope (IX-70, Olympus Corporation, Hachioji, Tokyo, Japan). Four representative fields within each section were randomly chosen and captured at 200X. The integrated optical density (IOD) in each image was measured with the same setting for all the slides, and the density was calculated as IOD/total area of each image.

TUNEL assay

After LPS-induced myocarditis, hearts were fixed in 4% paraformaldehyde in PBS for 24 h at room temperature. Fixed tissues were then embedded in a paraffin block, and 4-5 μm thick slices were cut from each tissue block. Immunohistochemical procedures for detecting apoptotic cardiomyocytes were performed by using an apoptosis detection kit (Boehringer Mannheim, Ridgefield, CT, USA) according to the manufacturer's instructions. Myocardial apoptosis was qualitatively analyzed by detection of DNA fragmentation (DNA ladders) and quantitatively analyzed by terminal dUTP nick end-labeling (TUNEL) assay as described previously [14]. Assays were performed in a blind manner.

Enzyme-linked immunosorbent assay

Enzyme-linked immunosorbent assay (ELISA) was used to quantify the cell culture supernatant levels of IL-1β, IL-6, TNFα, and iNOS. For the *in vitro* experimental assay, cells were pretreated with ATV (10 uM) in serum-free medium for 24 h at 37°C with 5% CO_2. Cells were then treated with LPS (100 ng/ml) in serum-free medium for 2 h at 37°C with 5% CO_2. After incubation, cells and the culture supernatant were collected into disinfected tubes. Mouse IL-1β ELISA (ab197742, Abcam), IL-6 ELISA (ab100-713, Abcam), TNFα ELISA (ab208348, Abcam) and iNOS ELISA (EK2328, SAB® Signalway Antibody) kits were used according to the manufacturer's recommendations. The absorbance at 450 nm was measured with an iMark Microplate Absorbance Reader (Bio-Rad).

Statistical analysis

Data are expressed as the mean ± SD from at least 4 independent experiments or 4 mice per group. Statistical significance was determined by one-way ANOVA with Bonferroni correction for multiple comparisons or by Student's unpaired *t*-tests. A *P* value < 0.05 was considered statistically significant.

Results

Levels of AKT2 phosphorylation and expression of SPK1, P-SPK1, P-MEK, and P-ERK are upregulated following LPS-induced macrophage migration

A transwell migration assay was performed using the murine macrophage cell line ANA-1. LPS induced macrophage migration was examined with micro Boyden analysis (**Figure 1A**). Protein levels of pan and phosphorylated AKT2, SPK1, MEK, and ERK were evaluated using Western

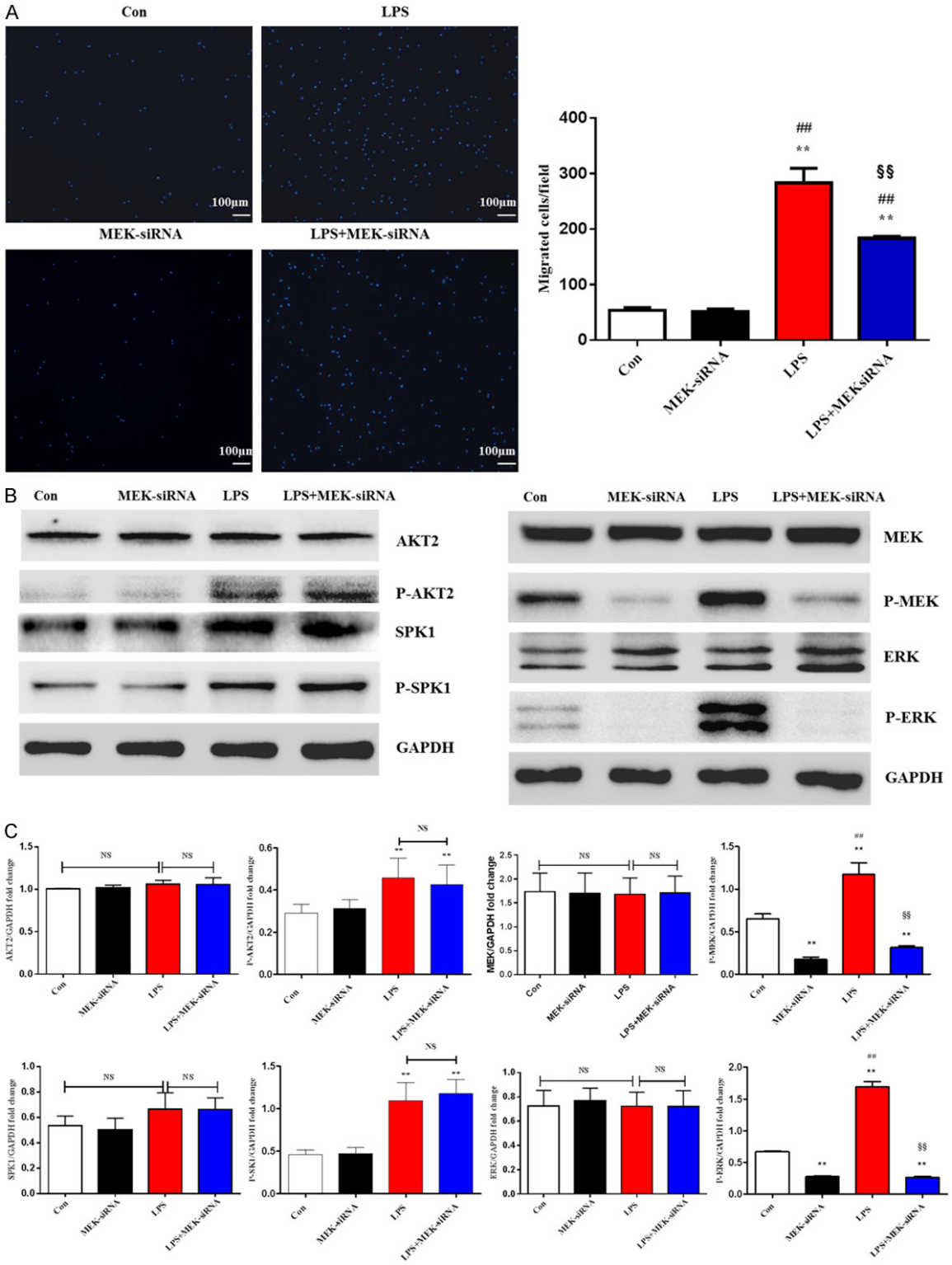

Figure 5. MEK-siRNA decreased ANA-1 cell migration and ERK and P-ERK protein expression, but had no effect on protein levels of AKT2, P-AKT2, SPK1, and P-SPK1. A. MEK-siRNA decreased migration of ANA-1 cells in a trans-well assay after LPS induction. ANA-1 cells were infected by LV-SPK1-siRNA, then cells were detached, and cell suspension (5×10^5 cells/ml) was placed in the upper well and serum-free RPMI 1640 medium with 100 ng/ml LPS was added to the bottom well. After 16 h of incubation, cells migrating across the membrane were stained and counted. The experiment was repeated three times. B. Protein expression in LPS and MEK-siRNA induced ANA-1 cells. Whole cell lysates were prepared following stimulation with LPS and MEK-siRNA. Immunoblots showed AKT2, P-AKT2,

SPK1, P-SPK1, MEK, P-MEK, ERK, P-ERK, and GAPDH protein expression levels. C. GAPDH normalized levels of AKT2, P-AKT2, SPK1, P-SPK1, MEK, P-MEK, ERK, and P-ERK. Data are presented as the mean ± SEM; n=3. *P < 0.05, **P < 0.01 compared with Con without LPS; #P < 0.05, ##P < 0.01 compared with MEK-siRNA group; §P < 0.05, §§P < 0.01 compared with Con+LPS induced group; NS = not significant.

blots. There was little difference in the expression levels of AKT2, SPK1, MEK, and ERK between unstimulated and LPS-stimulated macrophages. However, phosphorylation of AKT2, SPK1, MEK, and ERK and SPK1 was elevated (**Figure 1B** and **1C**).

Downregulation of AKT2 inhibits macrophage migration and protein expression levels of SPK1, P-SPK1

The association between AKT2 phosphorylation and expression of SPK1, MEK, and ERK was examined in LPS-challenged peritoneal macrophages isolated from WT and AKT2 KO (AKT2-/-) mice. Limited migration was observed in LPS-stimulated peritoneal macrophages isolated from AKT2-/- mice (**Figure 2A**). Levels of AKT2, P-AKT2, SPK1, and P-SPK1 decreased in macrophages from AKT2-KO mice. Little difference was observed in the expression levels of MEK, P-MEK, ERK, and P-ERK between unstimulated and LPS-stimulated macrophages. These data suggest that AKT2 phosphorylation may be an upstream signal for SPK1 and P-SPK1. P-AKT2 is unrelated to P-MEK and P-ERK protein expression.

Down-regulation of SPK1 impairs macrophage migration

To explore the role of SPK1 in LPS-induction, macrophage migration and levels of AKT2, P-AKT2, MEK, P-MEK, ERK, P-ERK, SPK1, and P-SPK1 were examined following SPK1-siRNA lentiviral infection. Decreased SPK1 protein expression with SPK1-siRNA inhibited macrophage migration (**Figure 3A**). SPK1-siRNA decreased SPK1 and P-SPK1 protein expression. There was no significant reduction in AKT2, P-AKT2, MEK, P-MEK, ERK, or P-ERK protein expression in LPS-induced macrophages treated with SPK1-siRNA. Notably, SPK1-siRNA significantly reduced the protein expression levels of SPK1 and P-SPK1, but not of SPK2 or P-SPK2, validating the specificity of SPK1-siRNA (**Figure 3B** and **3C**).

ERK inhibitor impairs macrophage migration

To explore the role of ERK in LPS-induction, macrophage migration and levels of AKT2, P-AKT2, MEK, P-MEK, ERK, P-ERK, SPK1, and P-SPK1 were examined following application of an ERK inhibitor. The ERK inhibitor limited macrophage migration (**Figure 4A**) and decreased ERK and P-ERK protein expression. However, there was no significant reduction in AKT2, P-AKT2, MEK, P-MEK, SPK1, or P-SPK1 protein expression in LPS-induced macrophages treated with the ERK inhibitor (**Figure 4B** and **4C**).

MEK-siRNA inhibits macrophage migration and ERK protein expression

Macrophage migration and levels of AKT2, P-AKT2, SPK1, P-SPK1, MEK, P-MEK, ERK, and P-ERK were examined following use of MEK-siRNA. MEK-siRNA limited macrophage migration (**Figure 5A**) and decreased ERK and P-ERK protein expression, but little difference was detected for AKT2, P-AKT2, SPK1, and P-SPK1 (**Figure 5B** and **5C**).

ATV inhibits macrophage migration associated with decreases in P-AKT2, SPK1, and P-SPK1, but ATV increased P-MEK and P-ERK protein expression in vitro

ATV has been reported to slow macrophage migration [13]. Here, we examined the effect of ATV on AKT2, P-AKT2, SPK1, P-SPK1, MEK, P-MEK, ERK, and P-ERK. ANA-1 cells were treated with ATV (10 μM) for 22 h prior to LPS (100 ng/ml) stimulation for another 2 h. The levels of AKT2, P-AKT2, SPK1, P-SPK1, MEK, P-MEK, ERK, and P-ERK were examined in ANA-1 cells. Our data revealed that ATV significantly suppressed macrophage migration (**Figure 6A**) as well as levels of P-AKT2, SPK1, and P-SPK1, without affecting AKT2 expression. ATV and LPS increased P-MEK and P-ERK protein expression. ATV increased P-MEK and P-ERK protein expression compared to that of ATV or LPS induced macrophages (**Figure 6B** and **6C**). ATV decreased the levels of Caspase 8, TNFα, IL-6, IL-1β, and iNOS (**Figure 6D**). Our data suggest that ATV suppressed macrophage migration through inhibiting the P-AKT2/SPK1 (P-SPK1) signaling cascade, and that P-AKT2/SPK1 (P-SPK1) may be the main cell signaling pathway in LPS induced macrophage migration.

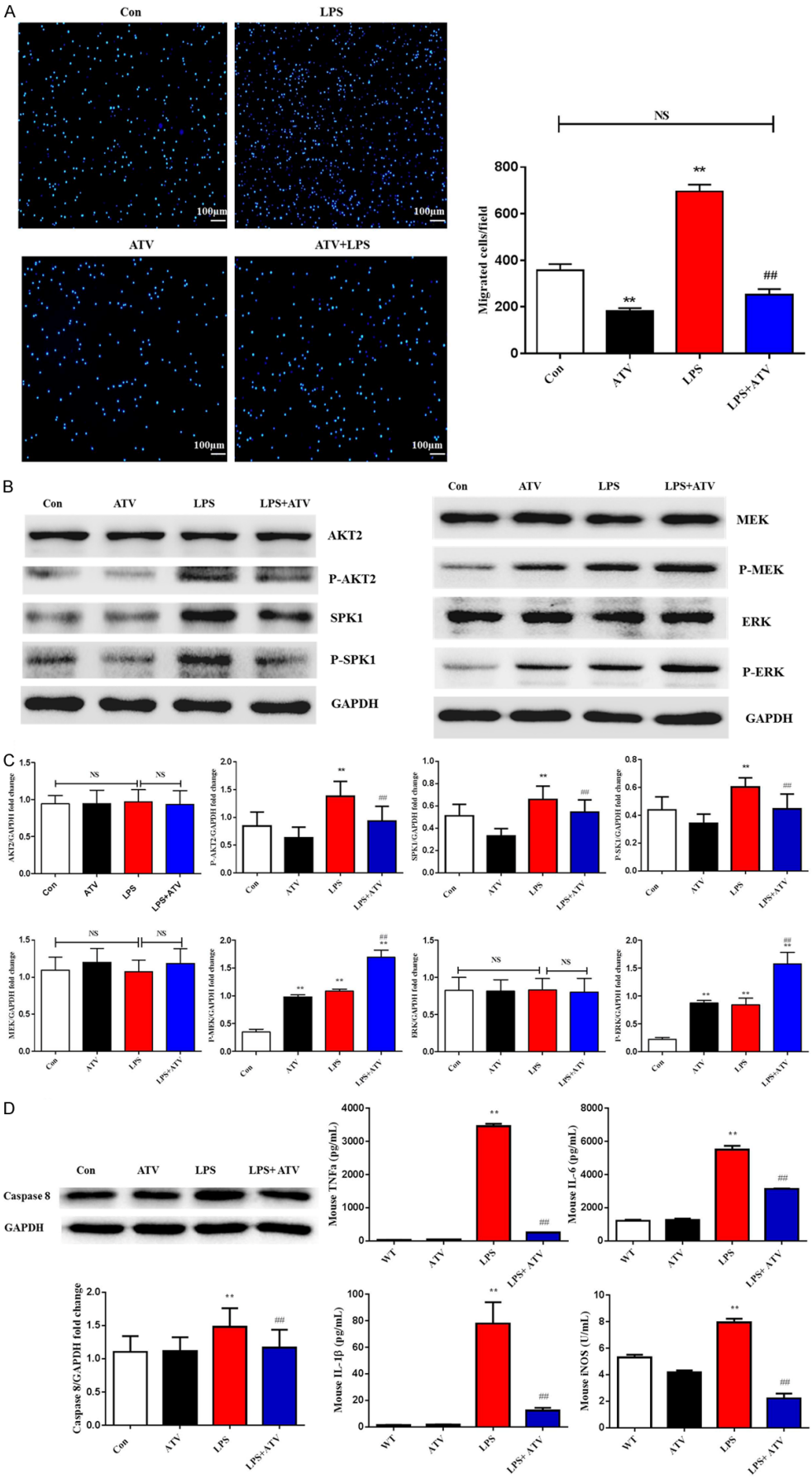
A
Con
LPS
ATV
ATV+LPS
100μm
NS
Migrated cells/field
B
Con
ATV
LPS
LPS+ATV
AKT2
P-AKT2
SPK1
P-SPK1
GAPDH
MEK
P-MEK
ERK
P-ERK
C
D
Caspase 8
Caspase 8/GAPDH fold change
Mouse TNFa (pg/mL)
Mouse IL-6 (pg/mL)
Mouse IL-1β (pg/mL)
Mouse iNOS (U/mL)
WT
LPS+ ATV

Figure 6. Atorvastatin (ATV) inhibits LPS-induced macrophage migration and protein expression of AKT2, P-AKT2, SPK1, and P-SPK1 in induced macrophages, but increased protein expression of MEK, P-MEK, ERK, and P-ERK. A. ATV decreases macrophage migration. ANA-1 cells were grown overnight and starved for 24 h and detached. Then, 5×10^5 cells were plated in the upper well and serum-free RPMI 1640 medium containing 100 ng/ml LPS with or without 10 μM ATV were added to the bottom well. Cells migrating across the membrane were stained and counted. The experiment was repeated three times. ATV decreases levels of AKT2, P-AKT2, SPK1, P-SPK1, Caspase 8, TNFα, IL-6, IL-1β, and iNOS, but increased P-MEK and P-ERK protein expression in LPS induced macrophages. ANA-1 cells were incubated with ATV (10 μM) for 24 h, then 100 ng/ml LPS induced ANA-1 cells for 2 h. Whole cell lysates were prepared. B. Immunoblots showed AKT2, P-AKT2, SPK1, P-SPK1, MEK, P-MEK, ERK, and P-ERK protein expression levels. C. GAPDH normalized levels of AKT2, P-AKT2, SPK1, P-SPK1, MEK, P-MEK, ERK, and P-ERK. D. ELISA and immunoblots results show the TNFα, IL-6, Caspase 8, IL-1β, and iNOS levels. Data are presented as the mean ± SEM; n=3. *P < 0.05, **P < 0.01 compared with Con without LPS; #P < 0.05, ##P < 0.01 compared with the Con+LPS induced group; NS = not significant.

ATV exerts cardiac protective effects by inhibiting macrophage recruitment, apoptosis, and inflammation factors

We also examined the role of SPK1 in WT and SPK1-/- animal models of LPS induced cardiomyopathy. Eight days after LPS-induced cardiomyopathy, the death rate was higher in WT than in SPK1-/- mice. 6 h after LPS induction, mice had bloody stools. Most WT mice died from infection and heart failure. ATV treatment increased survival rate in the LPS induced WT model, although it did not significantly lower the death rate of the SPK1-/- model (**Figure 7A**).

ATV treatment inhibited P-AKT2 protein expression in WT and SPK1-/- LPS-induced animals (P < 0.05). There was no significant difference in the levels of P-AKT2 between WT and SPK1-/- groups following LPS induced with and without ATV treatment (P > 0.05) (**Figure 7B** and **7C**). In contrast, macrophage density, apoptosis density, caspase 3 protein expression, the hypertrophy marker ANP, and expression of TNFα, IL-1β, and IL-6 were all significantly decreased in SPK1-/- LPS-induced animals compared with WT LPS-induced mice. In addition, the ATV treatment suppressed F4/80 protein expression (**Figure 7D**), apoptosis staining (**Figure 7E**), caspase 3 protein expression, the hypertrophy marker ANP, and TNFα, IL-6, and IL-1β expression in WT LPS-induced animals (**Figure 7F**). No significant difference was observed in SPK1-/- LPS-induced mice with and without ATV treatment compared with the WT.

There was a significant increase in fractional shortening and a marked decrease in LVEDD and LVESD 7 days after LPS-induction in SPK1-/- mice with or without ATV treatment compared with the WT. Echocardiographic analysis detected no obvious difference in fractional shortening, LVEDD, and LVESD in SPK1-/- mice with or without ATV treatment (**Table 1**).

Hemodynamic parameters also displayed a significant increase in +dP/dt and -dP/dt and decrease in LVEDP after LPS-induction in the SPK1-/- with or without ATV group compared with the WT. There was no significant difference in +dP/dt, -dP/dt, LVEDP, and HW/BW in SPK1-/- mice with or without ATV treatment (**Table 2**).

Discussion

Our study revealed that: 1) P-AKT2/SPK1 (P-SPK1) and MEK/ERK, two separate cell signaling pathways, were involved in LPS-induced macrophage migration; 2) P-AKT2/SPK1 (P-SPK1) plays a relatively important role compared to MEK/ERK cell signaling during macrophage migration; 3) ATV could inhibit P-AKT2/SPK1 (P-SPK1) cell signaling, but increase MEK/ERK cell signaling; 4) SPK1 may be harmful in LPS-induced myocarditis.

Results of the current study and previous findings [15], taken together, suggest that P-AKT2/SPK1 (SPK1) and P-MEK/P-ERK contribute to macrophage migration. However, we did not determine whether the P-AKT2/SPK1 (P-SPK1) and the P-MEK/P-ERK pathways acted in an independent or a interactive manner. In our previous study, we demonstrated that P-AKT2/NBA1/SPK1 regulates macrophage migration [15] and detected no difference in P-MEK and P-ERK protein level between WT, AKT2-KO, and SPK1-KO mice. Both MEK-siRNA and ERK inhibitor could inhibit macrophage migration. MEK-siRNA decreased ERK protein level, but MEK-siRNA did not affect the protein level of AKT2 and SPK1 (P-SPK1). The ERK inhibitor had no effect on MEK, P-MEK, P-AKT2, or SPK1 (P-SPK1) protein expression. We showed that the P-AKT2/SPK1 (P-SPK1) and the P-MEK/P-ERK pathways were involved in macrophage migration and acted in an independent manner.

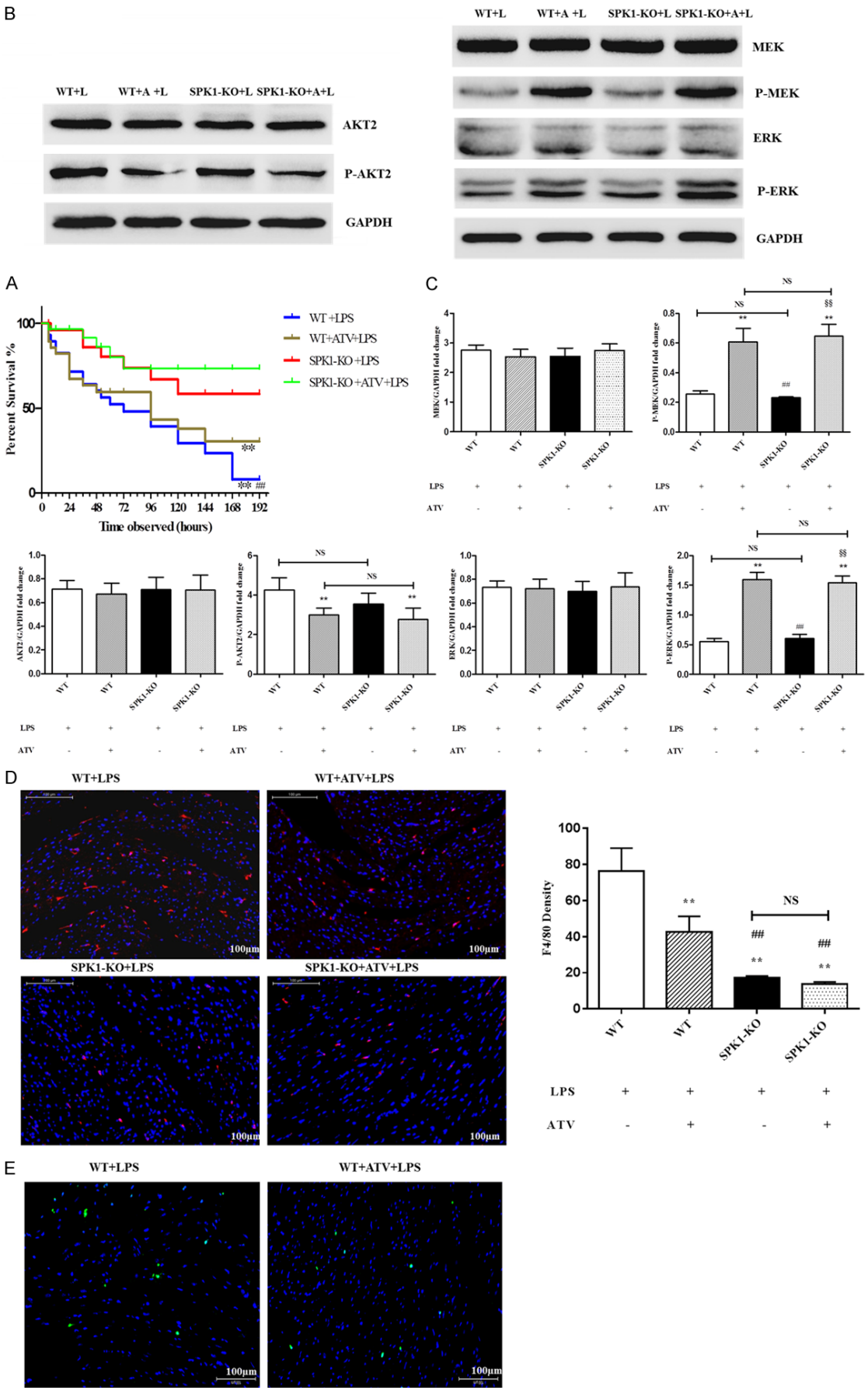
B
WT+L
WT+A +L
SPK1-KO+L
SPK1-KO+A+L
AKT2
P-AKT2
GAPDH
MEK
P-MEK
ERK
P-ERK
A
Percent Survival %
Time observed (hours)
WT +LPS
WT+ATV+LPS
SPK1-KO +LPS
SPK1-KO +ATV+LPS
C
MEK/GAPDH fold change
P-MEK/GAPDH fold change
AKT2/GAPDH fold change
P-AKT2/GAPDH fold change
ERK/GAPDH fold change
P-ERK/GAPDH fold change
LPS
ATV
NS
D
WT+LPS
WT+ATV+LPS
SPK1-KO+LPS
SPK1-KO+ATV+LPS
100μm
F4/80 Density
E
WT+LPS
WT+ATV+LPS
100μm

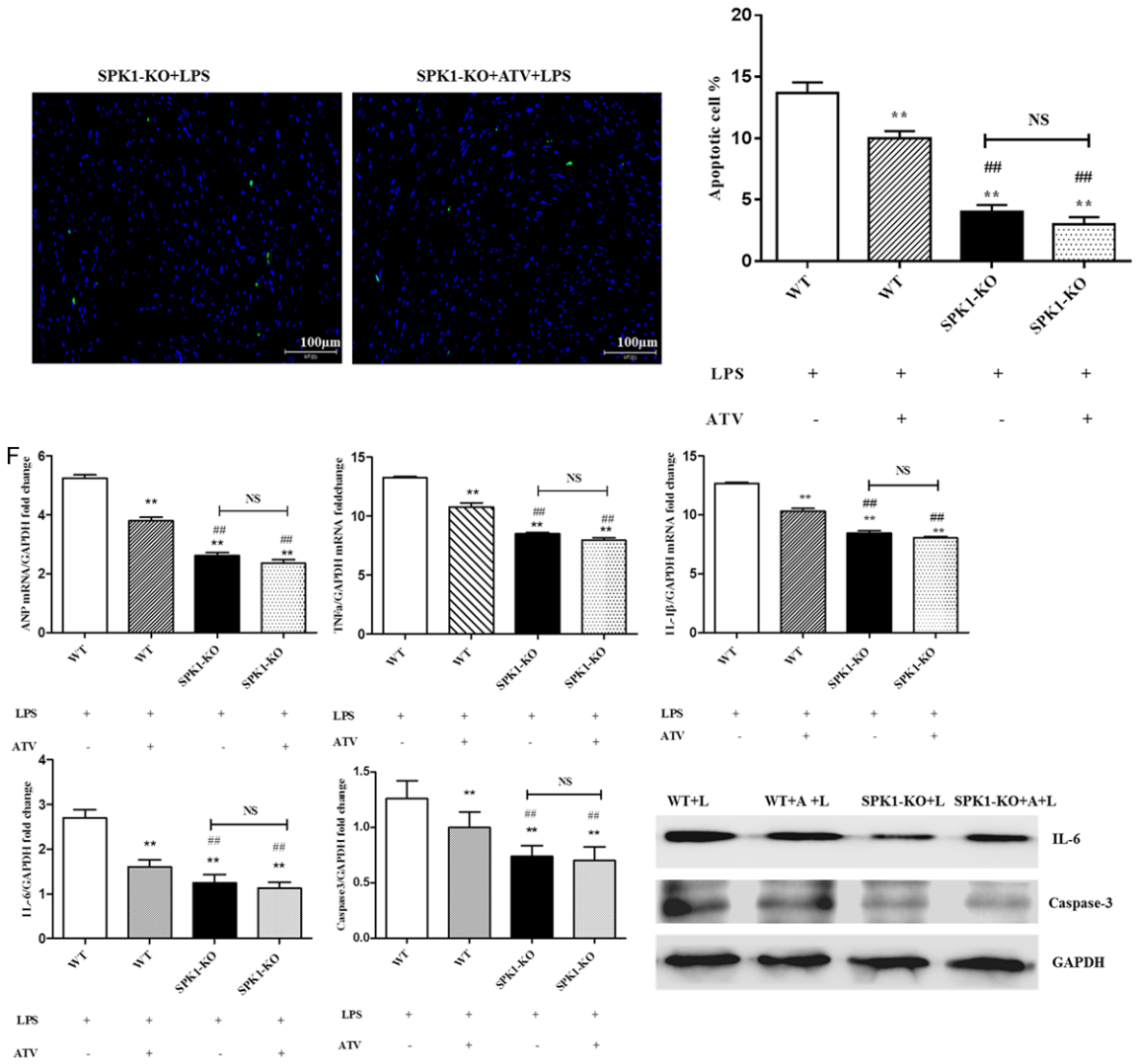

Figure 7. ATV protected cardiac function by reducing macrophage recruitment, apoptosis, TNFα, IL-1β, IL-6, and the survival curve, but the protective effect was dampened in SPK1-/- mice. WT and SPK1-/- mice were fed ATV (10 mg/kg/day) for 1 week before and after LPS induction. A. Survival curve for the WT LPS, WT+LPS+ATV, SPK1-/-+LPS, and SPK1-/-+LPS+ATV groups. 7 days after ATV and/or LPS induction, death rate of the WT+LPS group is higher than that of WT+LPS+ATV group. ATV treatment could decrease the death rate of WT+LPS model but did not lower the death rate of SPK1-/-+LPS models. *P < 0.05, **P < 0.01 vs WT LPS without ATV treatment group; #P < 0.05, ##P < 0.01 compared with the WT+LPS and ATV treatment group; ※P > 0.05 compared with the SPK1-/- without ATV treatment group. B, C. ATV could inhibit P-AKT2 protein levels in WT and SPK1-/- myocarditis animal model and could increase P-MEK and P-ERK protein levels. No difference was detected in AKT2, MEK, and ERK protein level between WT+LPS and SPK1-/-+LPS with and without ATV treatment. D. ATV could inhibit F4/80 density. E. ATV could inhibit apoptosis, F. ATV could inhibit ANP, TNFα, IL-1β, mRNA, IL-6, and Caspase-3 protein levels in the WT+LPS induced model. No difference in levels of F4/80 density, ANP, TNFα, IL-1β, IL-6, and Caspase-3 was detected in SPK1-/-+LPS-induced myocarditis model with and without ATV treatment. Data are presented as the mean ± SEM. *P < 0.05, **P < 0.01 compared with the WT+LPS group; #P < 0.05, ##P < 0.01 compared with the WT+LPS with ATV treatment group; NS = not significant.

Sepsis-induced myocardial injury (SIMI) is caused by various mechanisms. The administration of LPS to human volunteers results in a septic-like syndrome accompanied by decreased ventricular ejection fractions, biventricular dilatation, and altered cardiac index [16]. LPS may exert its effects by directly acting on cells, but also via downstream mediators including cytokines, adhesion molecules, nitric oxide, and reactive oxygen species. Sphingosine has been demonstrated to participate in the regulation of the cell cycle, apoptosis, and cal-

Table 1. Echocardiographic phenotypes of WT and SPK1-/- mice 7 days after LPS

	Group	FS%	LVEDD (mm)	LVESD (mm)	HR (beats/min)
LPS induced (n=15)	WT	26.63±1.37	4.06±0.09	3.22±0.06	448.1±5.93
	WT+ATV	32.10±1.09**	3.27±0.05**	2.99±0.03**	441.5±4.458
	SPK1-/-	40.48±0.57**,##	2.66±0.07**,##	2.52±0.03**,##	445.0±6.07
	SPK1-/-+ATV	41.12±0.70**,##,Δ	2.76±0.05**,##,Δ	2.42±0.03**,##,Δ	447.3±5.80

Data were obtained 7 days after LPS induction. FS%, percent fractional shorting; LVEDD, LV end-diastolic dimension in mm; LVESD, LV end-systolic dimension in mm; HR, heart rate. *P < 0.05; **P < 0.01 vs WT LPS; #P < 0.05, ##P < 0.01 vs WT+LPS+ATV; ΔP < 0.05 vs SPK1-KO+LPS.

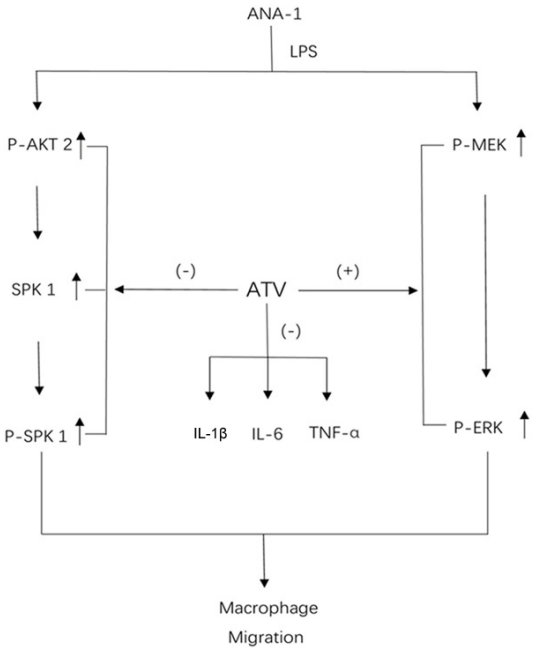

Figure 8. Model illustrating the mechanism of ATV-mediated LPS-induced myocarditis. P-AKT2/SPK1 (P-SPK1) is more important than P-MEK/P-ERK cell signaling in LPS-induced macrophage migration; SPK1 plays a harmful role in LPS-induced myocarditis. The mechanism of ATV protected cardiac function involves the inhibition of P-AKT2/SPK1 (P-SPK1) regulating macrophage recruitment, apoptosis, and the inflammation cytokines IL-1β, IL-6, and TNFα.

cium homeostasis. Two mammalian isoforms of sphingosine, SPK1 and SPK2, have been identified in the heart. SPK1 promotes growth and survival, whereas SPK2 may enhance apoptosis. Our previous study suggested that SPK1 is involved in macrophage migration, inflammatory cytokine secretion, and collagen deposition [15]. We showed that SPK1 is a beneficial cytokine in the myocardial infarction (MI) animal model [15]. In the LPS-induced myocarditis animal model, the SPK1-KO mice survival rate was higher than that of WT mice. Further, macrophage migration and levels of the cytokines IL-1β, IL-6, and TNFα were lower in SPK1-KO mice compared to WT mice. These findings suggested that SPK1 plays a harmful role in LPS-induced myocarditis animal model.

ATV produces greater benefits than expected from the reduction of lipid levels alone [17]. In our study, we showed that P-AKT2/SPK1 and P-MEK/P-ERK, two cell signaling pathways, acted separately in LPS-induced macrophage migration. ATV could inhibit macrophage migration by inhibiting P-AKT2/SPK1 (P-SPK1) cell signaling but could also increase P-MEK and P-ERK protein expression. In LPS-induced macrophage migration, the P-AKT2/SPK1 (P-SPK1) cell signaling pathway thus plays a more important role than does the P-MEK/P-ERK signaling pathway. The net effect of ATV is inhibition of macrophage migration. The P-AKT2/SPK1 (P-SPK1) signaling pathway is involved in LPS-induced macrophage migration. ATV protects cardiac function by inhibiting macrophage migration and the inflammation cytokines IL-1β, IL-6, and TNFα. This protective function of statins was partially attenuated in SPK1-KO mice.

In summary, our study demonstrated that P-AKT2/SPK1 (P-SPK1) is relatively more important than P-MEK/P-ERK cell signaling in LPS-induced macrophage migration. Second, SPK1 is harmful in LPS-induced myocarditis. Finally, the mechanism of ATV protection of cardiac function involves the inhibition of P-AKT2/SPK1 (P-SPK1), regulating macrophage recruitment, apoptosis, and the inflammation cytokines IL-1β, IL-6, and TNFα (**Figure 8**). Taken together, these observations suggest that SPK1 might be a novel therapeutic target to attenuate LPS-induced myocarditis.

Disclosure of conflict of interest

None.

Table 2. Organ weights and hemodynamics parameters of WT and SPK1-/- mice 7 days after LPS

	Group	HW/BW	+dP/d*t* (mmHg/s, Base)	+dP/dt (mmHg/s, ISO)	-dP/dt (mmHg/s, Base)	-dP/dt (mmHg/s, ISO)	LVEDP (mmHg/s, Base)	LVEDP (mmHg, ISO)
(n=15)	WT	4.23±0.05	5034±110.3	7433±55.51	-4487±72.56	-5075±54.87	13.16±0.25	13.96±0.12
	WT+ATV	3.68±0.05**	5133±96.62	9309±147	-5370±59.24**	-6344±56.65**	11.48±0.19**	12.01±0.30**
	SPK1-/-	3.26±0.019**,##	5028±101.7	10873±247.7**,##	-6186±34.96**,##	-7353±77.15**,##	8.81±0.32**,##	10.28±0.29**,##
	SPK1-/-+ATV	3.22±0.1**,##,Δ	5029±119.4	11270±272.1**,##,Δ	-6101±76.15**,##,Δ	-7181±78.15**,##,Δ	9.62±0.19**,##,Δ	10.72±0.31**,##,Δ

Base and 10 ng of isoproterenol (ISO) stimulated cardiac hemodynamic function were recorded. Data were obtained from mice 7 days after LPS induction. HW/BW: heart weight/body weight. +dP/dt and -dP/dt: maximal 1st time derivatives of left ventricular pressure rise and fall, respectively. LVEDP: LV end diastolic pressure. *P < 0.05; **P < 0.01 vs WT LPS; #P < 0.05, ##P < 0.01 vs WT LPS+ATV; ΔP < 0.05 vs SPK1-KO+LPS.

Address correspondence to: Lianyou Zhao and Xue Li, Department of Cardiology, Tangdu Hospital, Xi'an 710038, Shaanxi, China. E-mail: zhaoLyfmmu@126.com (LYZ); lxhlms@126.com (XL)

References

[1] Ma W, Wang Y, Lu S, Yan L, Hu F and Wang Z. Targeting androgen receptor with ASC-J9 attenuates cardiac injury and dysfunction in experimental autoimmune myocarditis by reducing M1-like macrophage. Biochem Biophys Res Commun 2017; 485: 746-752.

[2] Li X, Mikhalkova D, Gao E, Zhang J, Myers V, Zincarelli C, Lei Y, Song J, Koch WJ, Peppel K, Cheung JY, Feldman AM and Chan TO. Myocardial injury after ischemia-reperfusion in mice deficient in Akt2 is associated with increased cardiac macrophage density. Am J Physiol Heart Circ Physiol 2011; 301: H1932-1940.

[3] Shi Y, Lai X, Ye L, Chen K, Cao Z, Gong W, Jin L, Wang C, Liu M, Liao Y, Wang JM and Zhou N. Activated niacin receptor HCA2 inhibits chemoattractant-mediated macrophage migration via Gbetagamma/PKC/ERK1/2 pathway and heterologous receptor desensitization. Sci Rep 2017; 7: 42279.

[4] Allende ML, Sasaki T, Kawai H, Olivera A, Mi Y, van Echten-Deckert G, Hajdu R, Rosenbach M, Keohane CA, Mandala S, Spiegel S and Proia RL. Mice deficient in sphingosine kinase 1 are rendered lymphopenic by FTY720. J Biol Chem 2004; 279: 52487-52492.

[5] Cho H, Mu J, Kim JK, Thorvaldsen JL, Chu Q, Crenshaw EB 3rd, Kaestner KH, Bartolomei MS, Shulman GI and Birnbaum MJ. Insulin resistance and a diabetes mellitus-like syndrome in mice lacking the protein kinase Akt2 (PKB beta). Science 2001; 292: 1728-1731.

[6] Pineda-Torra I, Gage M, de Juan A and Pello OM. Isolation, culture, and polarization of murine bone marrow-derived and peritoneal macrophages. Methods Mol Biol 2015; 1339: 101-109.

[7] Jin ZQ and Karliner JS. Low dose N, N-dimethylsphingosine is cardioprotective and activates cytosolic sphingosine kinase by a PKCepsilon dependent mechanism. Cardiovasc Res 2006; 71: 725-734.

[8] Xu P, Yu H, Zhang Z, Meng Q, Sun H, Chen X, Yin Q and Li Y. Hydrogen-bonded and reduction-responsive micelles loading atorvastatin for therapy of breast cancer metastasis. Biomaterials 2014; 35: 7574-7587.

[9] Funakoshi H, Zacharia LC, Tang Z, Zhang J, Lee LL, Good JC, Herrmann DE, Higuchi Y, Koch WJ, Jackson EK, Chan TO and Feldman AM. A1 adenosine receptor upregulation accompanies decreasing myocardial adenosine levels in mice with left ventricular dysfunction. Circulation 2007; 115: 2307-2315.

[10] Tavener SA, Long EM, Robbins SM, McRae KM, Van Remmen H and Kubes P. Immune cell Toll-like receptor 4 is required for cardiac myocyte impairment during endotoxemia. Circ Res 2004; 95: 700-707.

[11] Pleger ST, Remppis A, Heidt B, Volkers M, Chuprun JK, Kuhn M, Zhou RH, Gao E, Szabo G, Weichenhan D, Muller OJ, Eckhart AD, Katus HA, Koch WJ and Most P. S100A1 gene therapy preserves in vivo cardiac function after myocardial infarction. Mol Ther 2005; 12: 1120-1129.

[12] Iwasaki K, Kojima K, Kodama S, Paz AC, Chambers M, Umezu M and Vacanti CA. Bioengineered three-layered robust and elastic artery using hemodynamically-equivalent pulsatile bioreactor. Circulation 2008; 118: S52-57.

[13] Shiraya S, Miyake T, Aoki M, Yoshikazu F, Ohgi S, Nishimura M, Ogihara T and Morishita R. Inhibition of development of experimental aortic abdominal aneurysm in rat model by atorvastatin through inhibition of macrophage migration. Atherosclerosis 2009; 202: 34-40.

[14] Liu HR, Tao L, Gao E, Lopez BL, Christopher TA, Willette RN, Ohlstein EH, Yue TL and Ma XL. Anti-apoptotic effects of rosiglitazone in hypercholesterolemic rabbits subjected to myocardial ischemia and reperfusion. Cardiovasc Res 2004; 62: 135-144.

[15] Yang Y, Zhao J, Zhang J, Lei Y, Yuan F, Liu L, Gao H, Guo H, Niu X, Chen R, Fu X, Han Y, Han H, Chan T, Zhao L, Wang H, Zheng Q and Li X. Regulation of macrophage migration in ischemic mouse hearts via an AKT2/NBA1/SPK1 pathway. Oncotarget 2017; 8: 115345-115359.

[16] Suffredini AF, Fromm RE, Parker MM, Brenner M, Kovacs JA, Wesley RA and Parrillo JE. The cardiovascular response of normal humans to the administration of endotoxin. N Engl J Med 1989; 321: 280-287.

[17] Yang N, Cheng W, Hu H, Xue M, Li X, Wang Y, Xuan Y, Li X, Yin J, Shi Y and Yan S. Atorvastatin attenuates sympathetic hyperinnervation together with the augmentation of M2 macrophages in rats postmyocardial infarction. Cardiovasc Ther 2016; 34: 234-244.